Examining the Role of Eyewall Convection in Hurricane Intensity Change Using Airborne Radar Observations

Annette M. Foerster and Michael M. Bell

Department of Atmospheric Sciences, University of Hawaii at Manoa, HI *Email: foerster@hawaii.edu*

1 Introduction

Forecasting tropical cyclone (TC) intensity remains challenging, because TC intensity is determined by many internal and external processes. Recent studies have suggested that the radial location of eyewall convection relative to the radius of maximum wind is an important component of intensification efficiency. However, our understanding of the physical processes, that potentially determine the location and strength of eyewall convection, such as eyewall buoyancy, is still incomplete.

2 Buoyancy Definition

Buoyancy is not defined uniquely. It depends on the choice of the reference state: $b = g\left[\frac{\theta'_v}{\theta_{v,0}} + (\kappa - 1)\frac{p'}{p_0} - q'\right]$

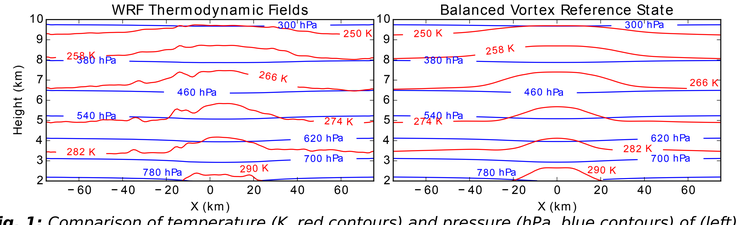

Fig. 1: *Comparison of temperature (K, red contours) and pressure (hPa, blue contours) of (left) a WRF vertical cross section, and (right) the balanced vortex retrieval calculation using the azimuthally averaged WRF wind field at 1800 UTC 20 September 2005.*

The most intuitive choice for a tropical cyclone reference state is a vortex in gradient wind and hydrostatic balance, because this subtracts off the bulk of the pressure gradient that balances the kinematic field and thus is not available to accelerate air parcels.

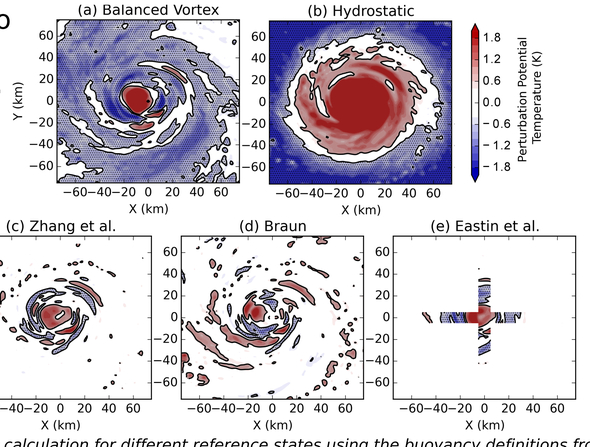

Fig. 2: *Buoyancy calculation for different reference states using the buoyancy definitions from previous studies, (a) a vortex in thermal wind balance, (b) a hydrostatic, horizontally uniform background state, (c) a locally averaged mean field (average over a box of 12-km x 12-km), (d) a low-wavenumber Fourier decomposition, and (e) a 20-km running mean along a flight track.*

3 Methodology

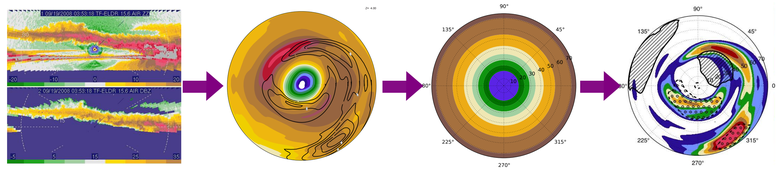

Fig. 3*: Schematic of the three-step process to derive buoyancy: (1) wind retrieval, (2) calculation of the reference state, and (3) thermodynamic retrieval.*

The retrieval infers pressure and temperature fields from kinematic measurements. It is based on existing thermodynamic retrievals (Gal-Chen, Roux, Liou), but modified to account for the horizontally non-uniform tropical cyclone environment.

$$\frac{\partial u}{\partial t} + u\frac{\partial u}{\partial x} + v\frac{\partial u}{\partial y} + w\frac{\partial u}{\partial z} - fv + c_p\bar{\theta}_\rho\frac{\partial \bar{\pi}}{\partial x} = A = -c_p\bar{\theta}_\rho\frac{\partial \pi'}{\partial x} - c_p\theta'_\rho\frac{\partial \bar{\pi}}{\partial x}$$

$$\frac{\partial v}{\partial t} + u\frac{\partial v}{\partial x} + v\frac{\partial v}{\partial y} + w\frac{\partial v}{\partial z} + fu + c_p\bar{\theta}_\rho\frac{\partial \bar{\pi}}{\partial y} = B = -c_p\bar{\theta}_\rho\frac{\partial \pi'}{\partial y} - c_p\theta'_\rho\frac{\partial \bar{\pi}}{\partial y}$$

$$\frac{\partial w}{\partial t} + u\frac{\partial w}{\partial x} + v\frac{\partial w}{\partial y} + w\frac{\partial w}{\partial z} = C = -c_p\bar{\theta}_\rho\frac{\partial \pi'}{\partial z} - c_p\bar{\theta}_\rho\frac{\partial \hat{\pi}}{\partial z} + g\frac{\theta'_\rho}{\bar{\theta}_\rho}$$

The last term in both horizontal momentum equations will be neglected. Scale analysis has shown that it is smaller than the equation's residual.

The wind field is derived from airborne Doppler data (complemented with dropsonde and flight level data) using SAMURAI (Bell et al., 2012).

The balanced vortex reference state is calculated using a method proposed by Smith (2006).

The thermodynamic retrieval is performed in two steps:
(1) pressure perturbations,
(2) temperature perturbations and pressure constants at each level.

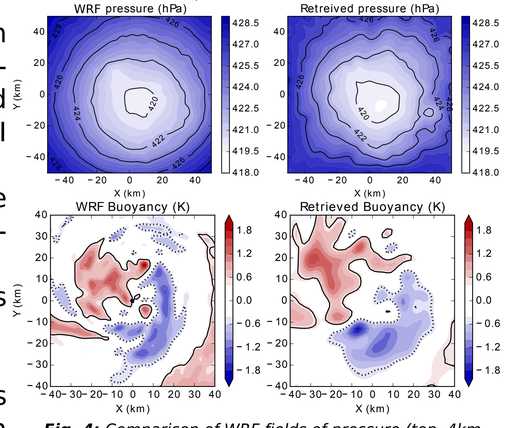

Fig. 4: *Comparison of WRF fields of pressure (top, 4km altitude) and buoyancy (bottom, 7.5 km altitude), and retrieved pressure and temperature perturbations for 18 UTC 21 September.*

Asymmetries in the eyewall convection pattern are associated with asymmetries in the radial and azimuthal location of buoyancy.

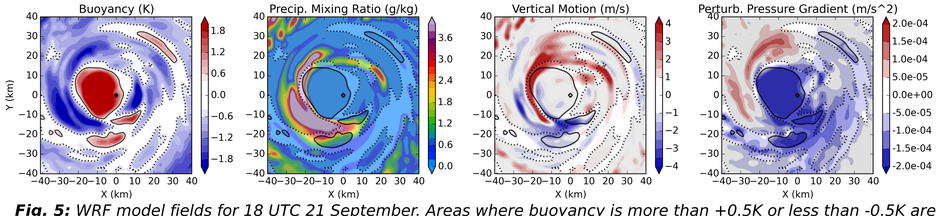

Fig. 5: *WRF model fields for 18 UTC 21 September. Areas where buoyancy is more than +0.5K or less than -0.5K are shaded gray, the thick solid line denotes the +0.5K buoyancy contour, the thick dashed line denotes the -0.5K buoyancy contour.*

4 Hurricane Rita (2005)

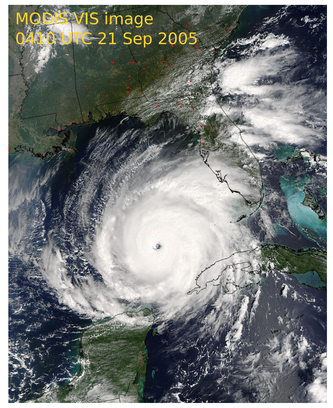

Fig. 6: *MODIS visible imagery of Rita at 0410 UTC 21 September 2005, when it was classified as a category 5 hurricane.*

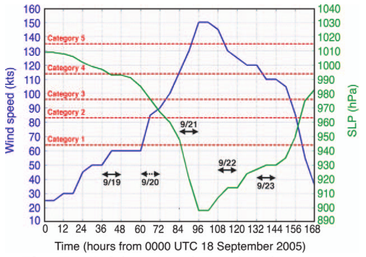

Fig. 7: *NHC best track sea level pressure (green) and wind speed (blue) for Rita (2005). Source: Houze et al. (2006).*

Airborne radar data of Hurricane Rita was collected by the NRL and the NOAA 42 and 43 P-3 aircraft as part of the RAINEX field campaign. Many changes in intensity and structure were observed, including rapid intensification, secondary eyewall formation and azimuthal asymmetries due to vertical wind shear.

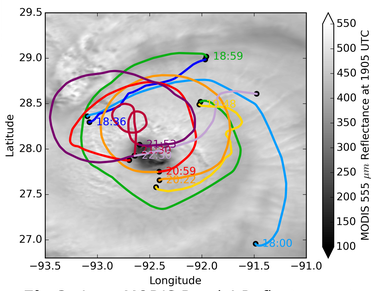

Fig 8: *Aqua MODIS Band 4 Reflectance at 1905 UTC 23 September 2005 overlaid with NRL P-3 flight track, broken up into nine flight legs for analysis purposes.*

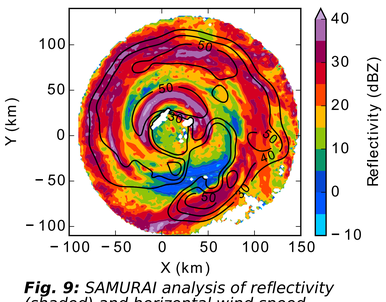

Fig. 9: *SAMURAI analysis of reflectivity (shaded) and horizontal wind speed (contours, m/s) at 2 km altitude derived from NRL P-3 data collected between 2022 UTC and 2059 UTC.*

5 Conclusions

Initial tests using a WRF simulation show the potential of the proposed retrieval technique to derive buoyancy fields from airborne radar observations in the inner core region of tropical cyclones. Careful analysis of the data collected in Hurricane Rita (2005) during five flights throughout its entire life cycle will help to identify and quantify the role of buoyancy in intensity change.

References: ***Bell, M. M., M. T. Montgomery, and K. A. Emanuel, 2012****: Air-Sea Enthalpy and Momentum Exchange at Major Hurricane Wind Speeds Observed during CBLAST. J. Atmos. Sci., 69, 3197–3222.* ***Braun, S. A., 2006****: High-Resolution Simulation of Hurricane Bonnie (1998). Part II: Water Budget. J. Atmos. Sci., 63, 43–64.* ***Eastin, M. D., W. M. Gray, and P. G. Black, 2005****: Buoyancy of Convective Vertical Motions in the Inner Core of Intense Hurricanes. Part I: General Statistics. Mon. Wea. Rev., 133, 188–208.* ***Gal-Chen, T., 1978****: A Method for the Initialization of the Anelastic Equations: Impliations for Matching Models with Observations. Mon. Wea. Rev., 106, 587–606.* ***Houze, R. A., Jr., J. Cetrone, S.R. Brodzik, S.S. Chen, W. Zhao, W.-C. Lee, J.A. Moore, G.J. Stossmeister, M.M. Bell, and R.F. Rogers, 2006****: The Hurricane Rainband and Intensity Change Experiment: Observations and Modeling of Hurricanes Katrina, Ophelia, and Rita. Bull. Amer. Meteor. Soc., 87, 1503–1521.* ***Roux, F., 1985****: Retrieval of Thermodynamic Fields from Multiple-Doppler Radar Data Using the Equations of Motion and the Thermodynamic Equation. Mon. Wea. Rev., 113, 2142–2157.* ***Smith, R. K., 2006****: Accurate determination of a balanced axisymmetric vortex in a compressible atmosphere. Tellus A, 58, 98–103.* ***Zhang, D.-L., Y. Liu, and M. K. Yau, 2000****: A Multiscale Numerical Study of Hurricane Andrew (1992). Part III: Dynamically Induced Vertical Motion. Mon. Wea. Rev., 128, 3772–3788.*